Int. J. Multiphase Flow, Vol. 5, pp. 1–15. Pergamon/Elsevier, 1979. Printed in Great Britain

CONDENSATION OF STEAM ON WATER IN TURBULENT MOTION

R. M. THOMAS
Central Electricity Research Laboratories, Leatherhead, Surrey, England

(*Received* 18 *May* 1978)

Abstract—An experimental study has been made of the rate at which steam condenses on a pool of turbulent water, under conditions where diffusion of heat in the liquid phase is the controlling factor. A variety of flow configurations have been examined, including a vertical jet impinging on the free surface from below, grid turbulence decaying in an open channel and recirculating flows generated by submerged horizontal jets. It was found that the theoretical model proposed by Theofanous, Houze & Brumfield (1976) provided a basis for correlating the results. In addition, the experiments on the vertical jet arrangement supported the prediction of Gardner & Crow (1973) that as agitation increases a condition is reached, characterized by a critical Kutateladze number, beyond which the condensation rate is considerably enhanced.

1. INTRODUCTION

The work reported here was undertaken with the objective of developing a way of estimating the rate at which steam condenses at the free surface of a body of cold water in turbulent motion. Studies of the condensation process are not only an essential preliminary to any attempt to quantify non-equilibrium effects in two-phase flows, but are also of more general interest insofar as they indirectly throw light on the structure of turbulence near a free surface.

Consider a pool of cold turbulent water covered by an atmosphere of steam. Provided the absolute pressure is not too low, the free surface will be very nearly at the steam temperature, and the rate of condensation will be determined by the rapidity with which heat can be transferred from the free surface to the bulk water. The simplest possible case is defined by four conditions: (i) the turbulence is so weak that the free surface remains essentially flat; (ii) the temperature difference between the steam and water is sufficiently small to ensure that there is negligible spatial variation of physical properties within the water pool; (iii) the density and viscosity of steam are small enough, and the steam velocities low enough, to permit neglect of dynamical coupling between phases; (iv) the latent heat is so large that the mass transfer associated with condensation has no influence on the structure of turbulence in the pool. The last two requirements will be met with good accuracy at absolute pressures near atmospheric; if the first two are also satisfied, dimensional analysis suggests that the heat transfer coefficient, K, defined as the heat flux per unit temperature difference between the steam and bulk water, will be expressible in the form

$$K = \frac{\kappa}{L} fn(Re_L, Pr),$$

where κ is the molecular conductivity, Re_L is a Reynolds number based on the pool length scale L, and Pr is the Prandtl number, $c_P\rho\nu/\kappa$; here, c_P, ρ and ν are respectively the specific heat, density and kinematic viscosity of water.

Any departure from the simplifying restrictions specified above renders the task of predicting the condensation rate considerably more difficult. If the water is much colder than the steam, the structure of the turbulence near the surface of the pool may possibly be modified as a result of a tendency towards stable density stratification and the fact that the viscosity of water is a strong function of temperature. At high pressures the density and viscosity of steam become appreciable, and flow patterns in the steam phase may then be expected to have some effect on

the motion of the free surface and hence on the condensation rate. Perhaps most important of all, when the turbulence intensity is high the free surface becomes violently agitated, giving rise to modes of heat transfer, such as the entrainment of steam bubbles, which have no counterpart in flows bounded by stationary surfaces.

As a first step towards a theoretical treatment, it seems useful to establish empirically the magnitude of the heat transfer coefficients associated with a variety of free-surface flows, so that a broad overall view can be obtained of the factors important in determining the condensation rate. The present experiments are in the nature of an exploratory investigation of this kind.

2. HEAT TRANSFER APPARATUS

2.1 *Vertical jets*

The experimental arrangement for the first set of condensation measurements is shown schematically in figure 1. A lagged glass test vessel, 0.30 m in diameter and about 0.6 m high, was maintained partially full of water during a run; the space above the free surface was continuously supplied with steam from a boiler, excess being discharged to atmosphere through a vent sufficiently large to ensure that the pressure in the test vessel did not significantly exceed ambient, but small enough to prevent the ingress of air. Water tapped from the boiler was cooled in a glass heat exchanger and pumped, via a control valve, through one of several interchangeable nozzles fitted into the base of the test vessel. Nozzles of diameter 3.18 mm, 6.35 mm and 12.7 mm were used. The residence time of water in the test vessel was of order tens of seconds, so the jets could be regarded as exhausting into essentially stagnant surroundings. Water leaving the test vessel through a drain in the base passed through a control valve and a cooler (to overcome cavitation problems), and was pumped back to the boiler.

Calibrated thermocouples were used to measure, within ±0.15°C, the temperature of the water entering and leaving the test vessel and of the steam. The nozzle flowrate was monitored, with an accuracy of about ±5%, by means of an inclined water-over-mercury manometer connected across a calibrated orifice plate in the feed pipe. A simple calculation shows that the mass of steam condensed per unit time was negligible in comparison with the nozzle flowrate, so the heat flux across the free surface could be calculated simply from these thermocouple and manometer readings. A scale attached to the outside of the test vessel permitted the depth of water to be read off directly, the free surface being visible through a slit in the lagging.

The steam flowrate was estimated from the approximately known power supplied to the boiler; a qualitative indication was also provided by the visual appearance of the jet of vapour emitted from the top of the test vessel. The heat transfer data were found to have no discernible dependence on the steam flowrate, and so no attempt was made to measure this parameter more accurately. Tests also showed that the position of the pipe through which steam was fed to the test vessel had no measurable influence on the results, confirming the view that resistance to heat transfer lay entirely in the water phase.

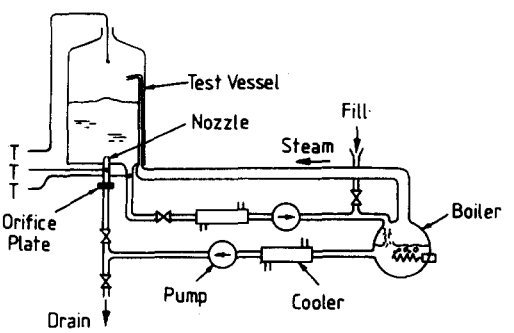

Figure 1. Vertical jet apparatus. Thermocouples marked T.

A run was carried out as follows. The heater in the boiler was switched on and the apparatus allowed to warm up, with the pumps circulating water, until steam was issuing freely from the vent. The inlet valve was adjusted to give the required nozzle flowrate and the outlet valve set to maintain a constant water level in the test vessel. The heat exchanger in the feed line was then adjusted to give the desired degree of cooling and, if necessary, the boiler power trimmed so that steam was issuing steadily from the test vessel. When conditions eventually became steady, the thermocouple readings and nozzle flowrates were recorded.

To estimate the magnitude of heat losses from the test vessel, several runs were carried out as described above with a raft of insulating material floating on the surface of the water pool. The outlet temperature was lower than the inlet temperature (the reverse of the usual situation), and knowledge of the difference between the two, together with the water flowrate, permitted the heat loss to be evaluated as a function of water depth. All the condensation data have been corrected in this way. The maximum loss was found to be less than 100 W, small in comparison with typical free-surface heat transfer rates of the order of a kilowatt.

2.2 *Horizontal flows*

When work on the vertical jet configuration had been completed, the experimental apparatus was extensively modified as shown in figures 2 and 3. An open channel of length 1.09 m and cross-section 100 mm × 100 mm, constructed from half-inch sheets of tufnol, was supported horizontally within an airtight, cylindrical glass vessel. Pipes passing through one of the end flanges fitted to the glass vessel allowed water to enter the channel in various ways. The water could be passed at relatively low velocity through a turbulence-promoting grid at the channel entrance, an arrangement which will be referred to as grid-channel flow, or introduced through one of a pair of

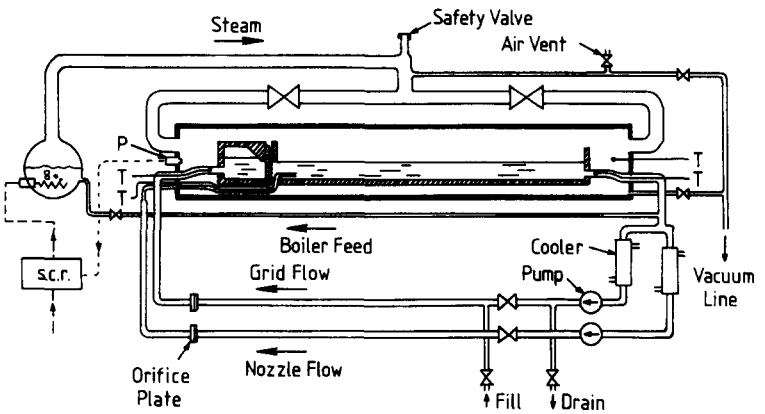

Figure 2. Horizontal channel apparatus. Thermocouples marked T, pressure transducer marked P. Downstream nozzle not shown.

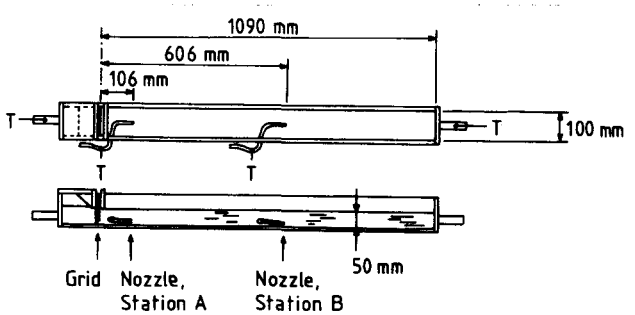

Figure 3. Channel details. Thermocouples marked T.

submerged nozzles. For all experiments the water level was maintained at 50 mm, with a tolerance of ±3 mm. The grid was of the usual square-mesh type, two rows of cylindrical bars, 6.35 mm in diameter and spaced at 12.7 mm centres, being fixed together at right angles. The nozzles, 4.51 mm in diameter, were directed horizontally along the channel centre line. One was situated 106 mm downstream from the channel entrance and the other at 606 mm; these will be called stations A and B respectively. Each nozzle was set 5 mm above the bottom of the channel, that is, 45 ± 3 mm below the free surface. For some experiments use was made of a submerged baffle consisting of a horizontal metal sheet 1.59 mm thick, perforated with 3.18 mm holes to give 40% free area; it covered the whole width and length of the channel and was supported 20 mm above the bottom of the channel.

Water left the channel through a pipe passing through the flange at the downstream end of the glass vessel, and was divided and returned to either the grid inlet or a nozzle inlet via one of two separate pipelines external to the vessel each of which included a heat exchanger, a glandless pump, a control valve and a standard orifice plate.

Steam generated in a boiler entered the glass vessel through two ports, one in each end flange. Power was fed to the boiler via a thyristor stack controlled by a circuit designed to keep the steam space at constant pressure, as sensed by a transducer fitted to the glass vessel. It was originally hoped that experiments carried out over a range of pressures would indicate the way in which condensation rate varied with the Prandtl number of the water very close to the free surface, but in fact any such dependence was lost in the scatter of the data. The two steam lines from the boiler were valved so that tests could be performed with steam entering the glass vessel at one end only; in this way it was possible to confirm that flow patterns in the steam space had no effect on the rate of condensation on water in the channel. Calculations also showed that conduction through the channel walls made a negligible contribution to the overall heat transfer.

Water flowrates were observed, within ± 5%, by means of water-over-mercury manometers connected across the orifice plates in the pipelines supplying the grid and nozzles. Temperatures were measured with an accuracy of ±0.15°C with thermocouples placed at the inlet and outlet of the channel and in the steam space; some tests were carried out with an additional thermocouple at a high position in the outflow pipe, to check that there was no significant stratification in the water leaving the channel. As was the case for the vertical jet experiments, the mass of steam condensed was very small, so that knowledge of the inlet and outlet temperatures and the water flowrate was sufficient to calculate the heat flux at the free surface.

At the beginning of each run the apparatus was filled with water to a level somewhat below that required and then evacuated. The boiler power was switched on and the steam pressure allowed to build up to a suitable value in the range 0.43 to 0.95 bar by adjusting the thyristor controller; lower pressures could not be obtained owing to difficulties caused by vapour locking in the pumps. The required flowrates were set and mains water added to bring the level in the channel to the specified level, without opening the vessel to atmosphere. Steady conditions were quickly reached, although it was found that small fluctuations in water temperature, of order ±0.3°C, tended to persist, probably as a consequence of imperfectly even running of the pumps; to minimize errors, therefore, ten sets of thermocouple readings were taken at one-minute intervals and the average, for each thermocouple, used in the subsequent calculations.

To combat the possible adverse effects of air blanketing the free surface, the test vessel was periodically connected to the vacuum line between runs so that water boiled vigorously from the channel. Accumulation of insoluble surface films was similarly minimized by regularly flooding the channel so that overflow occurred, renewing the free surface. The results of runs carried out immediately after these procedures showed no systematic differences from the results obtained immediately before, suggesting that errors due to the presence of air and surface contaminants were unimportant.

3. DETAILS OF THE EXPERIMENTAL FLOWS

Auxiliary experiments were carried out to determine the flow structure in the heat transfer apparatus described above. It is convenient to discuss these tests, which were carried out at ambient temperatures in the absence of condensation, before the heat transfer results are presented.

3.1 *Surface breakup*

It has already been mentioned that the proper interpretation of heat and mass transfer at a free surface requires an understanding of the circumstances in which bubbles of the supernatent phase are entrained. Simple tests were therefore performed on the vertical jet configuration to establish the condition for surface breakup.

A steel tank, 1.2 m × 1.2 m × 1.8 m high and fitted with Perspex windows, was partially filled with water. A nozzle fixed through the centre of the floor of the tank and directed vertically upwards was fed by a pump drawing water from two offtakes, also in the floor of the tank; a control valve was provided in the circuit and the flowrate measured, within ± 5%, by means of a manometer connected across a standard orifice plate. The control valve was initially opened fully, so that many air bubbles were being drawn down into the water, and then gradually closed until no bubble was observed over a continuous period of 30 s; the corresponding flowrate was then noted. This procedure was carried out for various depths of water in the tank and for two different nozzle diameters, 38.1 mm and 19.1 mm.

The results of these tests are shown in figure 4. The critical nozzle velocity for bubble entrainment appears to be roughly proportional to s/d, where d is the nozzle diameter and s, known as the submergence, is the distance of the nozzle below the free surface. This finding is in agreement with the proposal of Gardner & Crow (1973) that surface breakup occurs when the Kutateladze number exceeds a critical value:

$$\frac{\rho U_a^2}{(\Delta\rho g\sigma)^{1/2}} \geqslant \text{const.}, \qquad [1]$$

where U_a is the peak mean velocity at distance s from the nozzle in the absence of the free surface, $\Delta\rho$ is the density difference between phases and σ is the surface tension. For $s/d \geqslant 15$ the data of Wygnanski & Fiedler (1969) suggest the approximation

$$U_a = \frac{6.0\, U_n}{s/d},$$

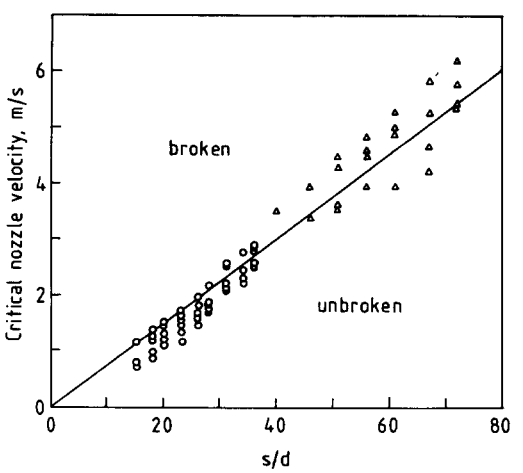

Figure 4. Threshold for surface breakup. ○, d = 38.1 mm; △, d = 19.1 mm.

where U_n is the nozzle velocity, so [1] yields as the condition for entrainment

$$U_n \geq 0.46 \frac{(\Delta\rho g\sigma)^{1/4}}{\rho^{1/2}} \frac{s}{d}, \qquad [2]$$

where the numerical value of the coefficient has been taken from the data of figure 4.

The present results for the critical nozzle velocity are about 50% higher than those obtained in a similar series of experiments by Higginbottom (1970). This discrepancy may be due to the comparatively crude lighting arrangements used here, which made it difficult to detect very small bubbles, or perhaps simply due to the fact that the present visual criterion for entrainment was less stringent than that of Higginbottom, who specified the absence of bubbles over a two-minute period. These uncertainties do not seriously impair the usefulness of [2] in discussing the condensation data presented in section 4.1.

3.2 *Anemometer measurements*

Constant-temperature hot-film anemometry was employed to obtain the mean velocity or turbulence intensity in several of the experimental flows. Cylindrical quartz-coated probes, 70 μm in diameter and 1.25 mm long, were calibrated on the basis of a King's law plot; the anemometer signal was linearized and turbulence intensities obtained by means of an analogue squaring circuit with a low-frequency cut-off at 0.01 Hz. The anemometer measurements were performed solely to guide interpretation of the condensation data, and no attempt was made to achieve very high accuracy, although care was taken to eliminate obvious sources of systematic error such as drift in water temperature and contamination of the probe.

Hot-film measurements on the vertical jet arrangement were carried out not in the heat transfer test vessel but in a separate tank, 0.44 m × 0.57 m × 0.47 m deep. The impinging jet gives rise to a central zone over which the free surface takes on the shape of a raised mound, surrounded by a relatively flat region of indefinite extent beneath which there is a developing radial boundary layer attached to the surface. Attention was concentrated on the outer zone, since it was considered that an adequate qualitative picture of the flow in the inner region could be inferred from information on axisymmetric jets directed against a solid wall given by, for example, Bradshaw & Love (1959), Schrader (1961) and Tani & Komatsu (1966). Figure 5

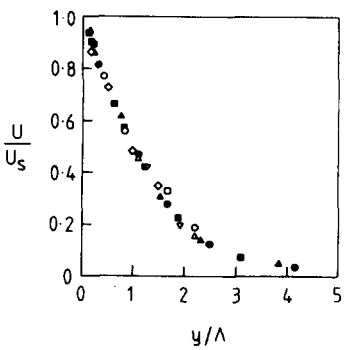

Figure 5. Mean radial velocity in the surface boundary layer.

	U_n, m/s	s, mm	r, mm
●	2.0	294	74
▲	2.0	294	99
■	2.0	294	150
○	1.0	214	72
△	1.0	214	97
□	1.0	214	148
▽	1.0	124	96
◇	1.0	124	147

shows the variation of mean velocity, U, with distance below the free surface, y, in the radial boundary layer, and figure 6 shows the way in which the radial surface velocity, U_s, and the boundary layer thickness, Λ, varies with distance from the centre of impingement, r; U_s has been estimated by extrapolating U to $y = 0$, and Λ has been defined as the depth at which the mean velocity is $\frac{1}{2}U_s$. It appears that for $r/s > 0.5$,

$$\frac{U_a}{U_s} = 2.3\frac{r}{s}; \qquad \Lambda = 0.045\, r.$$

The dependences $U_s \propto r^{-1}$ and $\Lambda \propto r$ are predicted by the analysis of self-preserving radial boundary layers given by Poreh *et al.* (1967). It is interesting that $\partial U/\partial y$, which must vanish at $y = 0$, attains high values within a very small distance of the free surface. This probably means that there is a thin viscous layer beneath the surface (Batchelor 1967, p. 364) within which $\partial^2 U/\partial y^2$ is large in comparison with its value in the fully turbulent zone accessible to the anemometer.

Experiments on the horizontal flow configurations were carried out in the heat-transfer channel, removed from its steam jacket. The r.m.s. fluctuating velocity signal, u, was measured by placing a sensor horizontally in the flow at right angles to the longitudinal axis, x, at a distance of 4 mm below the free surface. Although it is convenient to refer to u as the longitudinal turbulence intensity, it must be emphasized that no corrections have been applied (apart from the linearization itself) to allow for the high intensities occurring near the grid and in the recirculating flows induced by the horizontal jets. Bradbury (1976) has recently questioned the feasibility of extracting even qualitative information from hot-wire measurements in highly turbulent flows, and the plotted data should therefore be regarded with caution.

Figure 7 shows the results obtained for the case of water entering the channel via the grid. Near the grid, u is markedly non-uniform in the spanwise direction, z, as a result of the rather short settling length provided upstream. This inhomogeneity, together with the effect of the channel walls, leads to a decay of turbulence intensity quite different from that expected for simple grid flow (Batchelor 1953, p. 135).

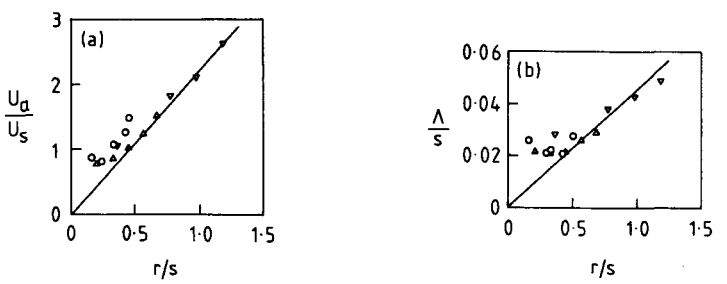

Figure 6. Radial free-surface boundary layer. (a) Variation of surface velocity. (b) Boundary layer thickness. ○, $s = 294$ mm; △, $s = 214$ mm; ▽, $s = 124$ mm.

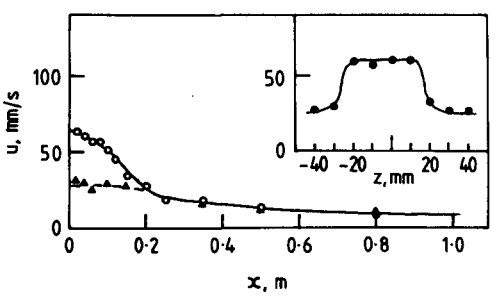

Figure 7. Longitudinal turbulence intensity: Grid-channel flow. $U_g = 100$ mm/s. ○, $z = 0$; △, average of values at $z = 40$ mm and $z = -40$ mm. Inset shows variation over channel width at $x = 40$ mm.

Figure 8 shows the levels of turbulence obtained with the horizontal jets. Visualizations by means of talc sprinkled on the free surface revealed that the jets set up a recirculating turbulent flow above and downstream of the nozzle. The effect of placing the perforated baffle plate over the jets is shown in figure 9. Backflow occurs over a proportion of the free surface, driven by the flow up through the baffle near the channel exit. The longitudinal turbulence intensity is only about 40% lower than in the unbaffled case.

The hot-film data for the various flows will be used in section 5 only as the basis for order-of-magnitude calculations. For this purpose, it is convenient to reduce the information contained in figures 5–9 to the grossly simplified form set out in table 1. For the grid-channel flow and horizontal jet flows, the variation of turbulence intensity over the free surface has been idealized by dividing the length of the channel into segments within which the intensity is taken to be constant, in such a way that the value of u averaged over the surface remains roughly the same as measured; a degree of subjective judgement is necessary in assessing the effect of spanwise inhomogeneity. For the vertical jet configuration, the turbulence intensity has been assumed to be 0.25 U_s, by analogy with free jets and wakes. It turns out that the integral scale of the turbulence, l, enters the calculation of condensation rate only as a factor $l^{-1/4}$, and so needs to be estimated only crudely. In the region adjacent to the grid, l has been taken equal to the mesh spacing, m. For the other horizontal flows, l has been equated to the depth of water in the channel, h; such a choice is prompted by the fact that talc visualizations reveal strong systems of large eddies at the free surface. In the radial boundary layer formed by the vertical

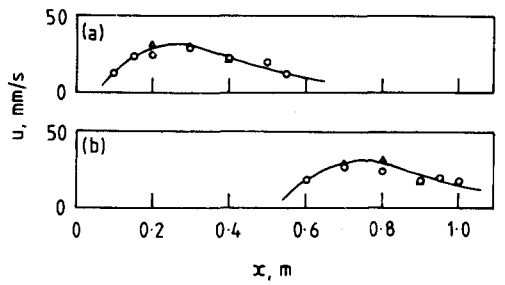

Figure 8. Longitudinal turbulence intensity: Horizontal jets. (a) Station A. (b) Station B. U_n = 2.0 m/s. ○, z = 0; △, average of values at z = 35 mm and z = −35 mm.

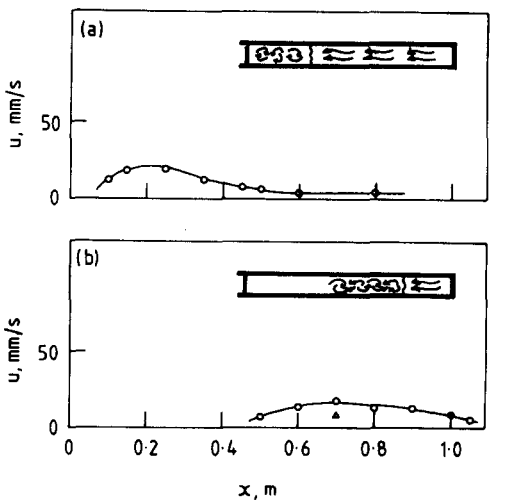

Figure 9. Longitudinal turbulence intensity: Baffled jets. (a) Station A. (b) Station B. U_n = 2.0 m/s. ○, z = 0; △, average of values at z = 35 mm and z = −35 mm. Insets show the flow patterns visible with talc dusted onto the free surface.

Table 1. Approximate velocity and length scales of the turbulence.

		u	l
Vertical jet	$0 < r < 0.3\,s$	$1.5\,U_n d/s$	$0.039\,s$
	$0.3\,s < r < R$	$0.65\,U_n d/s$	$0.045\,r$
Grid-channel flow	$0 < x < 0.15X$	$0.40\,U_g$	m
	$0.15X < x < X$	$0.15\,U_g$	h
Horizontal jets	over length $0.4\,X$	$0.012\,U_n$	h
	over length $0.6\,X$	0	—
Baffled jet, station A	over length $0.4\,X$	$0.008\,U_n$	h
	over length $0.6\,X$	$0.002\,U_n$	h
Baffled jet, station B	over length $0.6\,X$	$0.007\,U_n$	h
	over length $0.4\,X$	0	—

R is the radius of the test vessel used for the experiments on the vertical jet, X is the length of the horizontal channel and h is the depth of water in the channel.

jet, l has been identified with Λ; in the central impingement region, the integral scale has been taken to be that appropriate to a free jet, $0.039\,s$ according to Wygnanski & Fiedler (1969).

4. RESULTS OF THE CONDENSATION EXPERIMENTS

4.1 *Vertical jet*

For all the experiments on the vertical jet arrangement, the distance of the nozzle from the free surface was greater than 15 diameters, so that at impingement the jet consisted almost entirely of water entrained from the surrounding pool, which was assumed to be at a uniform temperature equal to that of the outflow from the test vessel. It was anticipated, therefore, that to good approximation the condensation rate would be proportional to the difference between the steam temperature and the outflow temperature. This expectation was confirmed within experimental error, and consequently the results will be presented in terms of an average heat transfer coefficient, $\langle K \rangle$, defined as the rate of flow of heat across the free surface per unit temperature difference between steam and outflow, divided by the total area of the free surface, $0.0707\ \mathrm{m}^2$.

Figure 10 shows the dependence of $\langle K \rangle$, for various water levels, on the nozzle Reynolds number, defined as

$$Re_n = \frac{U_n d}{\nu},$$

where U_n is the volumetric flowrate in the nozzle divided by its cross-sectional area. In calculating Re_n, the appropriate temperature for the evaluation of ν presents a difficulty. In the absence of any theoretical basis for rational choice, ν has been evaluated at the arithmetic mean of the steam temperature and the bulk liquid temperature. The matter seems to be of minor importance, as the reproducibility of the data is insufficient to reveal the effect of viscosity on the condensation rate: plots of $\langle K \rangle$ vs U_n differ little in appearance from figure 10, with similar scatter and slope.

The range of parameters covered by the experiments on the vertical jet and the other flows described below are set out in table 2.

For nozzle submergences greater than about 200 mm, $\langle K \rangle$ seems to be roughly proportional to Re_n. The appearance of the free surface in these cases is fairly quiescent, a gentle radial outward flow surrounding a central wandering stagnation point. At lower water levels the free surface becomes increasingly disturbed, a heaving mound of water several millimetres in height

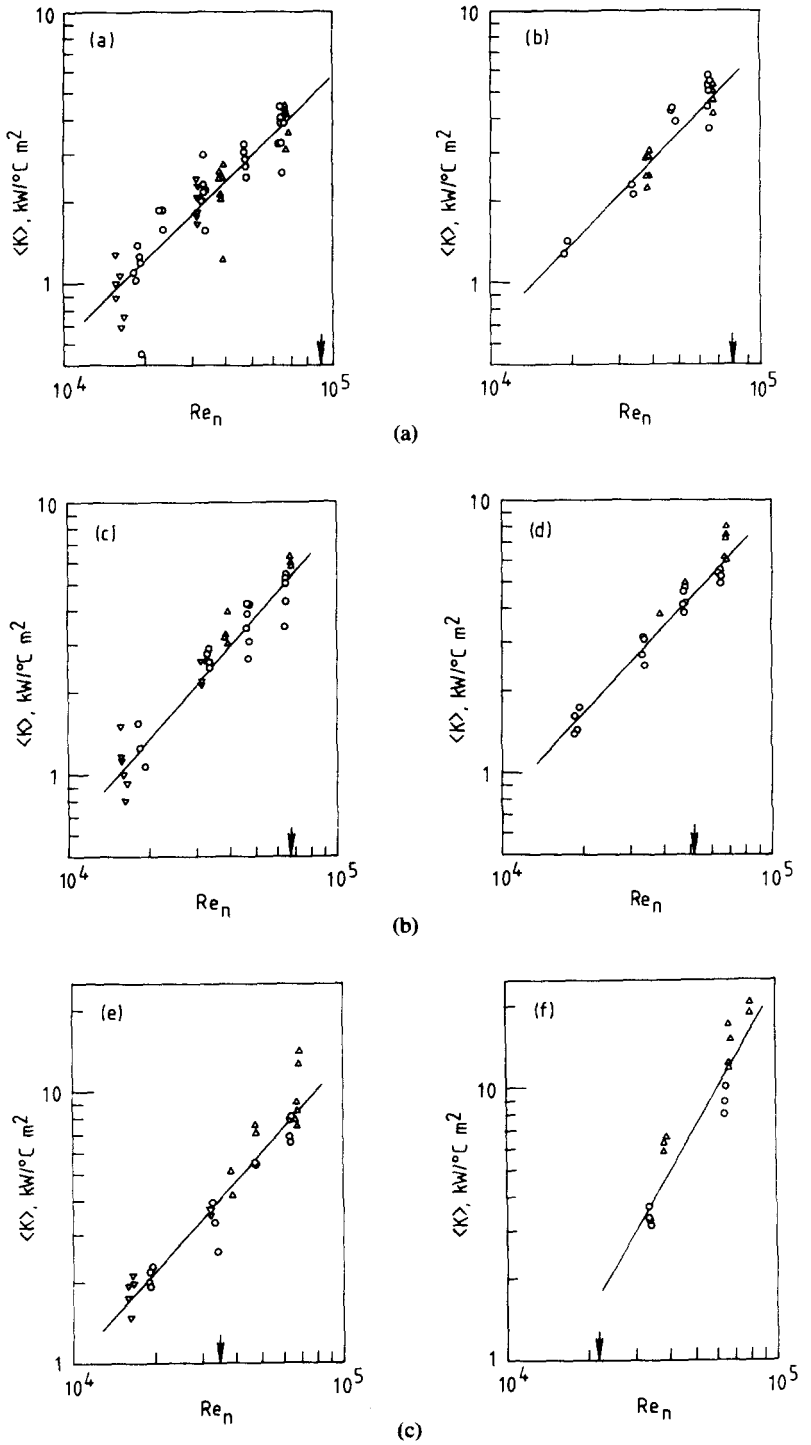

Figure 10. Heat transfer results: Vertical jet. (a) $s = 390$ mm; (b) $s = 340$ mm; (c) $s = 290$ mm; (d) $s = 220$ mm; (e) $s = 150$ mm; (f) $s = 95$ mm. Δ, $d = 3.18$ mm; O, $d = 6.35$ mm; ∇, $d = 12.7$ mm. Arrowheads indicate the condition for surface breakup.

being visible at the centre of impingement, and $\langle K \rangle$ begins to vary more rapidly with Re_n. This change in behaviour seems to be associated with the onset of surface breakup, the condition for which can be written, from [2],

$$Re_n \geq 0.46 \frac{(\Delta\rho g\sigma)^{1/4} s}{\rho^{1/2}\nu}. \qquad [3]$$

Table 2. Range of experimental parameters.

	U_n or U_g (m/s)		Re_n or Re_g, $\times 10^{-3}$		Outflow temp. (°C)		Prandtl number	
	min	max	min	max	min	max	min	max
Vertical jet, d = 3.18 mm	3.54	7.26	37.6	80.8	89.9	98.8	1.76	1.86
d = 6.35 mm	0.89	2.94	18.3	65.4	84.8	98.3	1.77	1.91
d = 12.7 mm	0.38	3.53	15.8	32.4	84.3	95.4	1.80	1.92
Grid-channel flow	0.016	0.117	0.531	4.44	29.9	79.0	2.01	3.33
Horizontal jets	1.32	1.87	17.1	25.2	61.0	72.5	2.10	2.26
Baffled jet, station A	1.11	1.67	13.4	23.7	52.5	80.2	1.99	2.36
Baffled jet, station B	1.11	1.67	13.2	22.9	52.5	73.7	2.07	2.40

This critical value of Re_n has been marked on figure 10; for simplicity the physical property parameters have been evaluated at the median temperature for the set of experiments on the vertical jet, 91.6°C. The trend of the condensation data clearly supports the idea that the criterion [3] describes a transition, albeit gradual, to a new heat transfer régime.

Under broken-surface conditions it is not necessarily the case that the heat flux depends linearly on the difference in temperature between the steam and bulk water, nor is it likely that the Reynolds number is an adequate characterization of the flow.

It may be noted that the measured heat transfer coefficients are sufficiently low to allow neglect of any temperature difference between the steam and the water surface, as estimated from kinetic theory (Collier 1972, p. 306); the same is true of the results for the other flow configurations examined.

4.2 *Horizontal flows*

As in the case of the vertical jet, the condensation rate for all the experiments in the horizontal channel was found to be directly proportional to the difference in temperature between the steam and the outflow water, permitting presentation of the data in terms of a heat transfer coefficient averaged over the area of the free surface, 0.109 m^2. The kinematic viscosity was again evaluated at the average of the steam temperature and the outflow temperature. The results showed no measurable dependence on absolute pressure. It is unlikely that the free surface was broken in the experiments on the horizontal flows; the criterion proposed by Gardner & Kubie (1976) for flows other than the vertical jet is similar to [1] but the approach velocity is replaced by a component of the turbulence intensity:

$$\frac{\rho u^2}{(\Delta\rho g\sigma)^{1/2}} \geq 3{\cdot}3\,. \qquad [4]$$

In the present experiments on grid-channel flow and the horizontal jets, the group on the left-hand side of [4] did not exceed 0.22 and 0.30 respectively.

The results for water entering the channel through the grid are displayed in figure 11; $\langle \dot{K} \rangle$ is plotted against the grid Reynolds number, defined as

$$Re_g = \frac{U_g m}{\nu}\,,$$

where U_g is the volumetric flowrate divided by the cross-sectional area of the channel flow, 5000 mm^2, and m is the mesh spacing, 12.7 mm. A least-squares fit to the data suggests that $\langle K \rangle$ is roughly proportional to Re_g, a dependence similar to that found for the vertical jets at large submergence. However, the scatter is sufficient to permit an alternative interpretation.

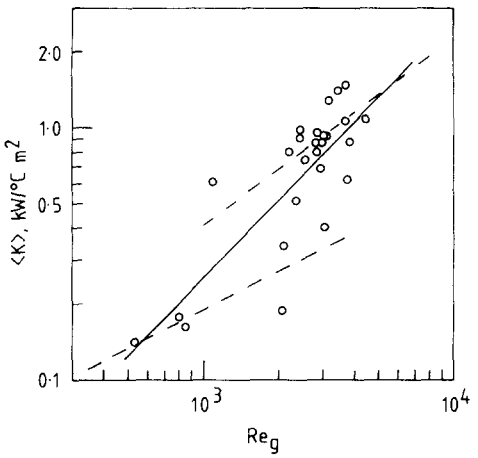

Figure 11. Heat transfer results: Grid-channel flow. Solid line: least-squares fit; broken line: see text.

Theofanous *et al.* (1976) have argued that free-surface mass transfer coefficients vary as $Re^{3/4}$ or $Re^{1/2}$ according as the turbulence Reynolds number, Re, is greater or less than a critical value of the order of a few hundred. For the grid-channel experiments, table 1 indicates that the turbulence Reynolds number is roughly 0.4 Re_g in the initial zone adjacent to the grid and 0.6 Re_g in the downstream zone, so that if the conclusions of Theofanous *et al.* are valid for heat transfer as well as mass transfer, it may be appropriate to regard the data points in figure 11 as falling into two separate categories, those at the lower left representing a $Re^{1/2}$ behaviour while the remainder correspond to the $Re^{3/4}$ dependence supposedly associated with fully-developed turbulence. The broken line drawn in figure 11 illustrates this possibility. The idea of two distinct heat-transfer régimes receives some support from the fact that the reproducibility of the measured heat-transfer coefficient was found to be especially poor for grid Reynolds numbers between 1000 and 2000, corresponding to Re in the ranges 400–800 in the initial zone and 600 to 1200 in the downstream zone, suggesting transitional behaviour. It is noteworthy that Bieber (1971) remarks that open-channel turbulence is not fully developed at Reynolds numbers, based on hydraulic diameter, below 8000, which corresponds in the present flow to a value of Re_g equal to 1016; however, anemometer observations showed the flow to be turbulent over the whole range of Reynolds numbers examined, so the change in heat-transfer régime (if real) is not the result of a simple laminar-turbulent transition.

Figures 12 and 13 show the results for respectively the low jets and the low jets covered by the perforated baffle. The data for the unbaffled jets are insufficient to allow the dependence of heat transfer coefficient on Reynolds number to be confidently inferred; the results for the baffled jets show the trend $\langle K \rangle \propto Re_n$.

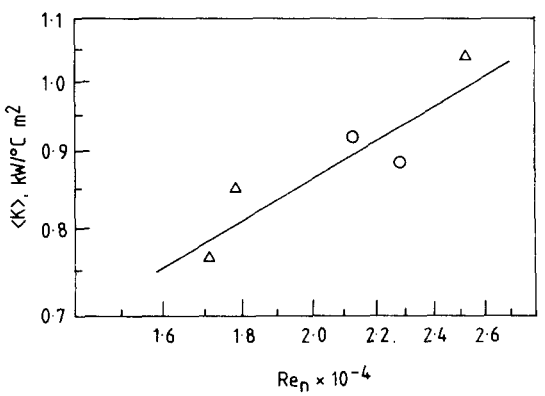

Figure 12. Heat transfer results: Horizontal jets. O, Station A; △, Station B.

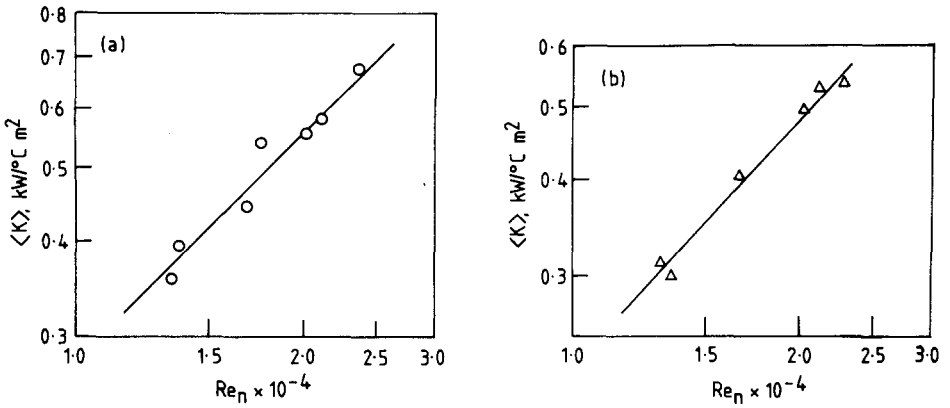

Figure 13. Heat transfer results: Baffled jets. (a) Station A. (b) Station B.

5. DISCUSSION

The results presented above may be interpreted with the aid of a simple two-layer model. It will be supposed that immediately adjacent to the free surface there is a layer, of small thickness δ, within which fluid motions are strongly influenced by viscosity; the thermal resistance of this layer will be described in terms of a heat transfer coefficient χ, so that a temperature drop Q/χ appears across it when the heat flux is Q. Beneath the viscous layer, it will be assumed that the eddy diffusivity for heat is of the form $\gamma c_P \rho u y/l$, where y is the distance from the free surface and γ is a constant of order unity. A simple calculation then shows that the overall heat transfer coefficient, K, is given by

$$K = \frac{\chi}{1 + \dfrac{\chi}{\gamma c_P \rho u} \ln\left(\dfrac{al}{\delta}\right)} \qquad [5]$$

where it has been assumed that the bulk temperature is attained at a distance al from the free surface.

The analysis of oscillatory free-surface boundary layers by Longuet-Higgins (1953, 1960) suggests that

$$\delta = b\left(\frac{\nu l}{u}\right)^{1/2}$$

where b is another constant of order unity. Hence [5] becomes

$$K = \frac{\chi}{1 + \dfrac{\chi}{\gamma c_P \rho u}(B + \ln Re^{1/2})} \qquad [6]$$

where $B = \ln(a/b)$ and $Re = ul/\nu$.

To complete the specification of the model, an estimate of χ is required. If the Prandtl number were very large, all the resistance to heat transfer would lie in the viscous layer; it follows that χ can be inferred from published information on free-surface mass-transfer processes, for which the Schmidt number (the analogue of the Prandtl number) is large and the concentration boundary layer very thin. The relevant mass-transfer data have recently been discussed by Theofanous *et al.* (1976); a slight generalization of their treatment yields

$$\chi = 0.25 \frac{\kappa}{l} Re^{3/4} Pr^{1/2} \qquad [7]$$

Table 3. Summary of the experimental results.

	Slope of plots of log $\langle K \rangle$ vs log Re_n or log Re_g	$\langle c_P \rho u \rangle$ (kW/°C m²)	$\langle \chi \rangle$ (kW/°C m²)	Measured $\langle K \rangle$ (kW/°C m²)
Vertical jet, s = 390 mm	0.988	255	6.97	2.86
s = 340 mm	1.056	288	8.06	3.56
s = 290 mm	1.126	323	9.19	3.78
s = 220 mm	1.069	370	10.71	4.31
s = 150 mm	1.115	418	12.27	6.22
s = 95 mm	1.741	455	13.50	7.20
Grid-channel flow	1.040	52	1.56	0.664
Horizontal jets	0.609	32	0.77	0.9
Baffled jet, station A	1.028	23	0.79	0.516
Baffled jet, station B	1.100	24	0.70	0.442

$\langle c_P \rho u \rangle$ has been evaluated at the median value of u: χ has been evaluated, and the measured $\langle K \rangle$ quoted, at the median values of Re and Pr.

for values of Re in excess of a few hundred. Table 3 shows the results of the present experiments together with the magnitudes of $c_P \rho u$ and χ. For all the tests $\chi \ll c_P \rho u$, so [6] predicts $K \approx \chi$. The experimentally observed values of K are indeed of the same order as χ, as calculated from [7]. However, K seems to vary nearly linearly with Re, rather than showing the expected $Re^{3/4}$ dependence. It is possible to speculate on the reasons for this discrepancy, but there is little point in doing so: more detailed experiments are clearly needed.

6. CONCLUSIONS

The main outcome of the work reported here may be summarized as follows.

(i) The magnitude of the free-surface heat transfer coefficient is predicted within a factor of two or three by a simple model derived from the work of Theofanous *et al.* (1976). However, the condensation rate shows a stronger variation with Reynolds number than the expected $\frac{3}{4}$-power dependence.

(ii) The experiments lend some support to the prediction of Gardner & Crow (1973) that a considerable increase in the rate of condensation occurs when the agitation of the free surface becomes sufficiently severe to cause entrainment of steam bubbles, a condition characterized by the attainment of a critical value of the Kutateladze number.

Acknowledgement—Mr. D. R. Wakeford and Mr. H. S. Oates assisted with some of the experiments. The work was carried out at the Central Electricity Research Laboratories and is published by permission of the Central Electricity Generating Board.

REFERENCES

BATCHELOR, G. K. 1953 *The Theory of Homogeneous Turbulence.* Cambridge University Press.

BATCHELOR, G. K. 1967 *An Introduction to Fluid Dynamics.* Cambridge University Press.

BIEBER, A. G. 1971 Absorption of a gas into a liquid in open channel flow. Ph.D. Thesis, Virginia State University.

BRADBURY, L. J. S. 1976 Measurements with a pulsed-wire and a hot-wire anemometer in the highly turbulent wake of a normal flat plate. *J. Fluid Mech.* **77**, 473–497.

BRADSHAW, P. & LOVE, E. M. 1959 The normal impingement of a circular air jet on a flat surface. ARC R & M 3205.

COLLIER, J. G. 1972 *Convective Boiling and Condensation.* McGraw-Hill, New York.

GARDNER, G. C. & CROW, I. G. 1973 Onset of entrainment with a jet directed at a two-phase interface. *Chem. Engng J.* **5**, 267–273.

GARDNER, G. C. & KUBIE, J. 1976 Flow of two liquids in sloping tubes. *Int. J. Multiphase Flow* **2**, 435–451.

HIGGINBOTTOM, D. 1970 Gas entrainment modelling of flows in which a free surface is disturbed by a jet of liquid directed from below. CEGB Note RD/B/N 1845.

LONGUET-HIGGINS, M. S. 1953 Mass transport in water waves. *Trans. Roy. Soc.* **A245**, 535–581.

LONGUET-HIGGINS, M. S. 1960 Mass transport in the boundary layer at a free oscillating surface. *J. Fluid Mech.* **8**, 293–306.

POREH, M., TSUEI, Y. G. & CERMAK, J. E. 1967 Investigation of a turbulent radial wall jet. *Trans Am. Soc. Mech. Engrs J. Appl. Mech.* 457–463.

SCHRADER, H. 1961 Trocknung feuchter Oberflachen mittels Warmluftstrahlen. VDI-Forschungsheft 484.

TANI, I. & KOMATSU, Y. 1966 Impingement of a round jet on a flat surface. *Proc. 11th Int. Congress Appl. Mech., Munich*, 672–676.

THEOFANOUS, T. G., HOUZE, R. N. & BRUMFIELD, L. K. 1976 Turbulent mass transfer at free, gas-liquid interfaces, with applications to open-channel, bubble and jet flows. *Int. J. Heat Mass Transfer* **19**, 613–624.

WYGNANSKI, I. & FIEDLER, H. 1969 Some measurements in the self-preserving jet. *J. Fluid Mech.* **38**, 557–612.